Hysteretic Characteristics of Long-Span Gravity-Load-Designed RC Frames with Masonry Infill Walls under Lateral Loading

Surasak Niyompanitpattana[1], Kerkrit Promduang[2], Jensak Kochanin[3], Amnart Khampanit[4], Pennung Warnitchai[5] and Sutat Leelataviwat[6]
Faculty of Industrial Technology, Ubon Ratcahthani Rajabhat University[1]
Department of Civil Engineering, King Mongkut's University of Technology[2, 4, 6]
Faculty of Industrial Technology, Uttatadit Rajabhat University[3]
School of Engineering and Technology, Asian Institute of Technology[5]
E-mail: surasak6791@gmail.com[1]

Abstract

A series of quasi-static cyclic loading tests on long-span gravity-load-designed RC frames with and without masonry infill walls is described. Test specimens with high aspect ratio are half-scale models of typical school buildings in Thailand. Five test specimens comprise one bare frame and four frames with either a full infill, partial-height infill, central-opening infill or side-opening infill. In this study the load-deflection relationship, strength, stiffness, ductility, energy dissipation capacities, and cyclic degradation of the test specimens are examined and compared partially with those of infilled RC frames with low-to-moderate aspect ratio.

Keywords: GLD Frame, Hysteretic Characteristic, Masonry Infill Wall, RC frame

1. Introduction

In many countries, masonry infill walls are normally constructed as external envelope walls and internal partitions of Gravity-Load-Designed (GLD) buildings. During ground motions, the interaction between these infill walls and RC frames can lead to unexpected or undesired effects when compared with the response of the bare frames, at both global and local levels. In terms of global level, the seismic performance of the structure can be greatly improved by the increase of lateral strength arising from the infill walls. On the contrary, this increase in lateral strength is also accompanied with the increase of initial lateral stiffness of the structures, and thus may results in an adverse increase of the inertia force [1]. The seismic damage of the structure may be reduced by dissipating a considerable portion of the input energy in the infill walls or at the interface between the infill walls and their surrounding frame members [2,3]. But if the distribution arrangement of infill walls is irregular, either in vertical profile or in plan or both, they can induce significant global damage to the structures such as torsional building response [4] and formation of soft-storey sidesway mechanism [5, 6]. Such storey-level sidesway mechanism can be formed even in buildings with uniform distribution of infill walls after the failure of infill walls in some storey [7].

The presence of infill wall also creates certain local interactions between the wall and its bounding frame members and may lead to local failures of these interacting components. Some of these infill-frame local interactions, such as highly concentrated stress in wall at the load corners and high shear load in frame members resulting from infill 'diagonal strut action'

near the load corners. There are many other effects of local interactions that need to be considered. For example, the 'diagonal strut' effect of infill wall not only increase shear forces but also can greatly affect the bending moments and axial forces in the interacting columns [8]. In the frame with partial-height infill wall, the 'short column' effect can be created and resulted in a significant increase in column shear forces [9].

Most of the past studies on frame-infill interaction are limited to those with low to moderate aspect ratio—the ratio of bay width to clear story height less than 2.0. Based on a database of 51 experiments from 24 different studies on RC frames with masonry infill walls compiled by Turgay [10], about 95% of experiments were conducted on specimens with aspect ratio between 1.2 and 2.0. There are, however, a large number of existing GLD buildings made of infilled RC frames with high aspect ratio (> 2.0). Some of them are schools and hospitals. The situation clearly indicates the need for more studies, especially experimental ones, for infilled frames with high aspect ratio, as shown in this paper.

In this paper, brief descriptions of test specimens are first present. Then load-deflection relationship is examined. Finally, hysteretic characteristics in term of strength, stiffness, ductility, energy dissipation capacities, and cyclic degradation of test specimens are also evaluated.

2. Experimental program

The prototype structure for this study was an interior infill frame on the first floor of a typical five-story school building in Thailand. The beam span of the frame is rather long – about 2·7 times the column height. The building was designed following an old version of the Engineering Institute of Thailand's design standard for RC buildings, EIT 1007-34. Neither seismic loads nor seismic detailing were considered in the design process of this building.

The test specimens used were half-scale models of the prototype infill frame. To ensure seismic similarity between the models and the prototype, the specimens were designed such that their key non-dimensional structural indices governing their seismic behavior and failure mechanism were nearly identical to those of the prototype, as shown in Table 1. Material tests were conducted on concrete, reinforcing steel and masonry samples, as shown in Table 2. Important geometrical dimensions, structural details, nonseismic reinforcement details and instrumentations of the test specimens are shown in Figures 1.

A lateral cyclic force was applied to each specimen by means of a servo-controlled hydraulic actuator with a force capacity of 500 kN and a maximum stroke length of 1000 mm (Figure 2). A constant axial load of 150 kN was applied through a setup consisting of a steel beam placed on the column top and two hydraulic jacks anchored to pin supports at the floor by two high-strength steel rods of 16 mm diameter. The cyclic loading test was displacement controlled, with each specimen forced to deform in a cyclic manner with stepwise increasing target drifts (Figures 2). This cyclic loading protocol was based on the recommendation of FEMA 461 [11]. Furthermore, at any target drift greater than 1·0%, where significant damage was expected, one small cycle of 0·2% drift was added to check the degradation of lateral stiffness of the specimen. The full details and descriptions of test specimens can be found elsewhere [12].

Table 1 Structural indices of prototype frame and test specimen

Structural indices	Column		Beam	
	Prototype	Model	Prototype	Model
Shear span ratio a/h	4.833	4.833	6.417	6.417
Normalized nominal flexural-to-shear strength M_n/aV_n	0.547	0.557	0.407	0.380
Longitudinal reinforcing index $\rho = A_s/(b_w d)$	0.037	0.034	0.025	0.022
Longitudinal reinforcing index $\rho' = A'_s/(b_w d)$	0.037	0.034	0.025	0.022
Transverse steel index $\rho_s\sqrt{b"/s}$	0.008	0.009	0.013	0.012
Normalized associated shear force index $V_a/(b_w d\sqrt{f'_c})$	1.293	1.264	0.768	0.662
Axial force ratio $P/(f'_c A_g)$	0.317	0.317	-	-

Table 2 Strength of materials

Properties (unit: MPa)	SP1	SP2	SP3	SP4	SP5
Concrete compressive strength of column	17.9	23.6	21.7	22.1	22.7
Concrete compressive strength of beam	20.3	27.9	22.5	23.1	24.1
Yield strength of DB 16	282.6	382.6	382.6	382.6	382.6
Yield strength of RB 6	373.6	373.6	373.6	373.6	373.6
Yield strength of Plain mild steel ϕ-3mm	392.4	392.4	392.4	392.4	392.4
Compressive strength of brick unit		8.5	8.5	8.5	8.5
Compressive strength of mortar		12.8	15.7	16.6	15.9
Compressive strength of plaster		7.7	13.7	23.8	20.1
Compressive strength of masonry[1]		5.9	7.7	10.6	8.5
Concrete compressive strength of tie beam/tie column		15.1	15.2	15.9	17.6

[1] Test specimen of size 150 x 150 cut from the infill wall after the test was complete

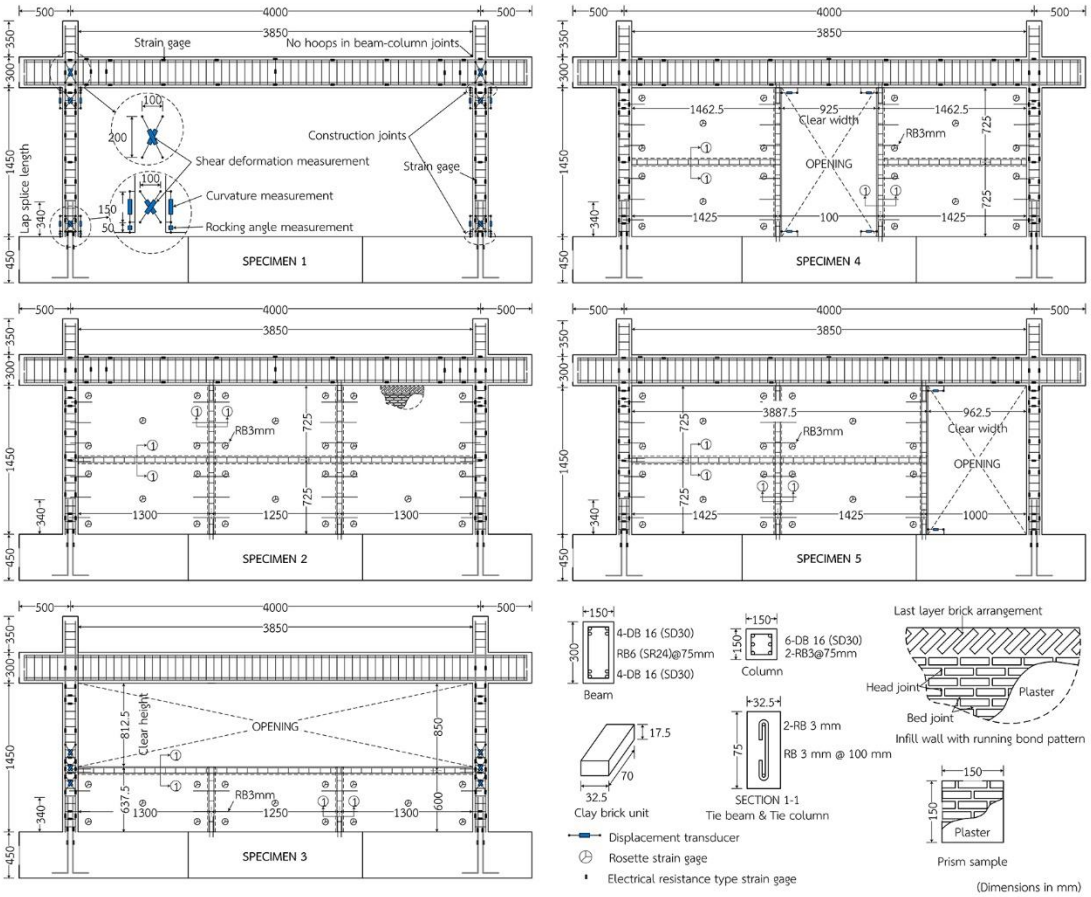

Figure 1 Structural details and instrumentation of test specimens (dimensions in mm)

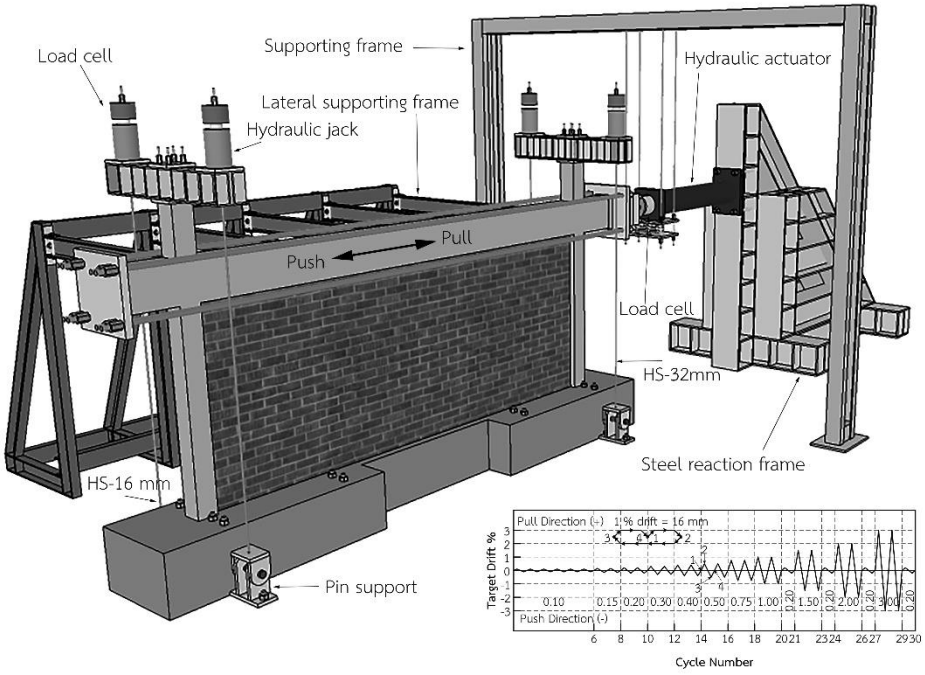

Figure 2 General test setup and Pattern of lateral cyclic displacement

3. Experimental results and discussion

3.1 Force - Drift Relationship

The relationship between lateral force and lateral displacement (drift) of specimen 1 is shown in Figure 3(a). Overall, this specimen shows the lowest lateral strength and stiffness compared with other specimens. This was expected since there is no strength and stiffness contribution from infill wall. The lateral force reaches the maximum values of 54kN (pull) and -52kN (push) at about 2.00–3.00% drift. The deformation of this bare frame is mainly concentrated in the columns, as the column size and flexural strength are much smaller than those of beam (strong beam-weak column). The deformation of columns is of flexural type as clearly indicated by very low strain level in transverse bars and much higher strain level in longitudinal bars. Throughout the test, the strains of column longitudinal bars at the lap-splice region (lower end) have never exceeded half of yield strain level, indicating a poor force-transfer mechanism in the lap-splice zone. The strains in the beam are also very low—less than ±600 micro strain—and no noticeable cracks are observed, indicating that the beam remains essentially elastic.

The lateral force-displacement relationship of specimen 2, as presented by Figure 3(b), shows much higher lateral strength and stiffness compared to the bare frame specimen. This result confirms the importance of infill wall in terms of its significant contribution to the lateral strength and stiffness. The lateral strength reaches its peak value of 162 kN (pull) and -170kN (push) at about 0.60—0.75% drift. The maximum strength of this specimen is about 2.98-3.25 times that of specimen1 (Table 3). As compared with infilled frame with aspect ratio of about 1.5-2.00 [13, 14], drift at maximum load of fully infilled frames is about 0.21-0.75. It seems drift at maximum load may not depends very much on the aspect ratio of the bounding frame. As the drift further increases, the strength gradually degrades, and the cyclic force-deformation relationship displays hysteretic loops with increasing ‘pinching’ effect. At the end of the test at drift greater than 2.0%, the degraded strength is still higher than + 100 kN, which is much greater than that of the bare frame (see also Figure 3 (f)).

For specimen 3, the presence of a partial-height infill wall substantially modifies the lateral response behavior of the frame by restraining lateral displacement in the lower half of the columns. The deformation of the frame is, therefore, concentrated in the upper half of the columns (short captive columns), as confirmed from visual observations and crack patterns (Figure 4(c)). At a low drift level, the lateral strength and stiffness of this specimen were slightly higher than those of specimen 1 but lower than those of specimen 2. The lateral strength reached a peak value of 72 kN (pull) and −65 kN (push) at about 1·00–1·50% drift. The hysteretic behavior up to this drift level was quite similar to that of the bare frame. As the drift further increased, the lateral strength degraded significantly (to a level below that of specimen 1) and some pinching effects in the hysteretic loops were observed, suggesting that the failure mechanism might be a non-ductile type.

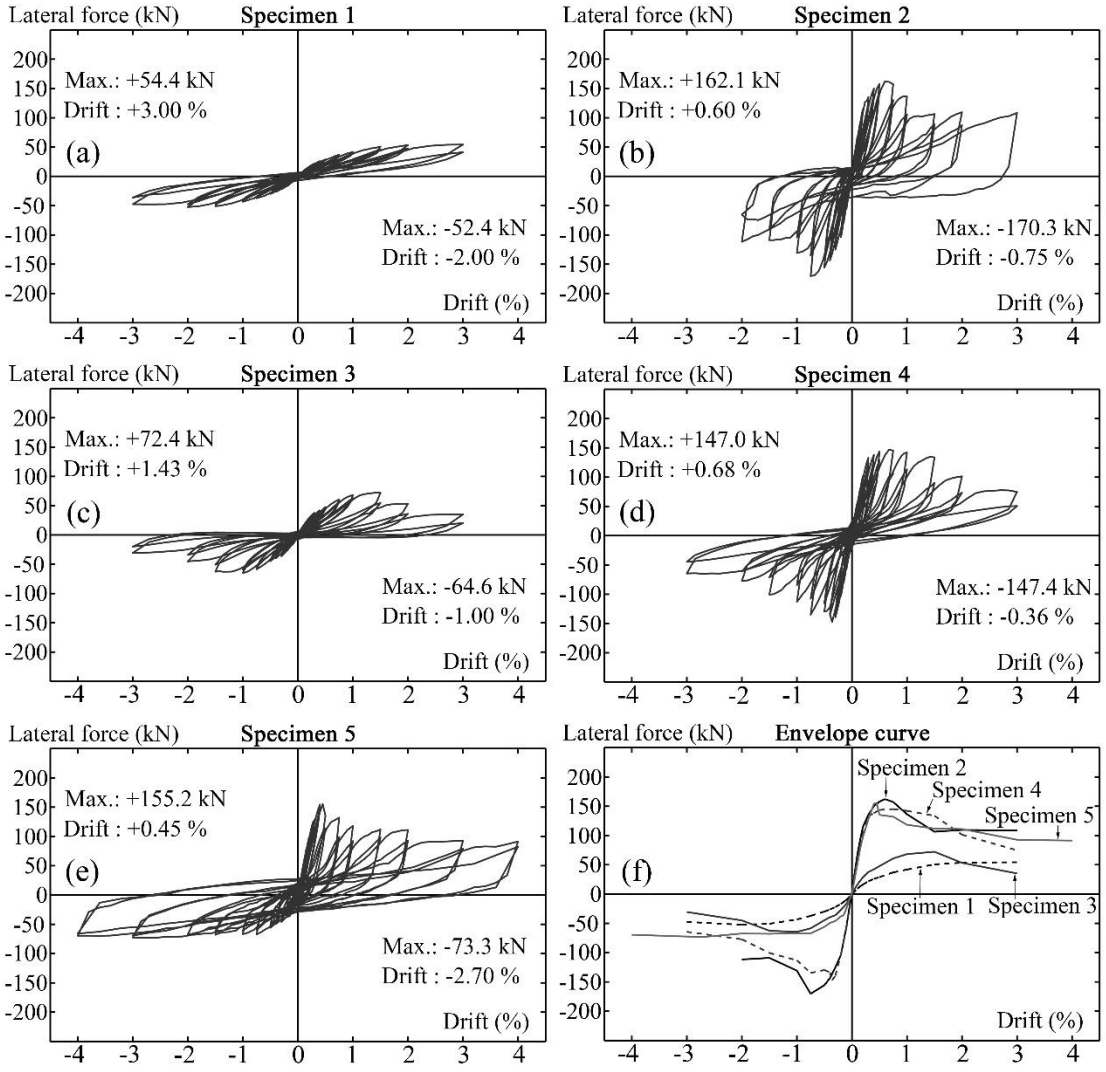

Figure 3 Lateral force-drift and envelope curve of test specimens

The lateral strength and stiffness of specimen 4 (Figure 3(d)) were comparable to, but not as high as, those of specimen 2. This suggests that a large central opening does not reduce much the significant contribution of infill to both the lateral strength and stiffness of the frame. The lateral strength of this specimen reached peak values of +147 kN (pull) and −147 kN (push) at about 0·40–0·75% drift. The maximum strength of this specimen is about 2.70-2.81 times that of specimen1 (Table 3). At higher drift levels, the lateral strength and stiffness degraded gradually. However, the residual strength at about 2·00–3·00% drift was still higher than that of the bare frame. Its hysteretic behavior was also similar to that of specimen 2.

For specimen 5, the most outstanding feature of this frame with a side-opening infill wall was its unsymmetrical force–deformation behavior. In the pulling phase, the lateral strength, stiffness and hysteretic behavior were similar to those of specimen 2, and the lateral strength reached a peak value of 155 kN at a low drift level of about 0·45%. The maximum strength of this specimen is 2.86 times that of specimen1 in this pulling phase (Table 3). This is due to the infill wall is actively engaging with the frame only when it pushed by the frame during the pulling

phase. In the pushing phase, the lateral strength, stiffness and hysteretic behavior were similar to those of specimen 1, and the lateral strength reached a peak value of 73 kN at a high drift level of about 2·0–3·0.

3.2 Ductility

From the lateral force-drift envelope curves in Figure 3(f), the ductility is defined as the ratio between the drift on the ascending branch and the descending branch of the envelope curve that corresponding to 85% of the maximum load; as shown in Table 3. This drift level can be considered as the ultimate limit state because this is the drift at which the degradation of the structural resistance begins to accelerate in most of the infilled frames [15]. Due to the drop of lateral strength to 85% of its peak value is not identified; the ductility of the specimen 1 is not shown in Table 3. For all infilled frames, the ductility factor is about 2.23-5.95. The maximum ductility for the infilled frames is founded in the specimen 4. This may be due to the infill slip, resulting in a gradual drop of the lateral strength of the whole system. For specimen 5, due to the same reason as specimen 1, the ductility is not defined in the push direction. As compared with the infilled frames with aspect ratio 1.5 in the study of Kakaletsis [15], the ductility is about 3.20-5.83. It seems that the ductility may not depend on the aspect ratio of the bounding frame.

3.3 Energy Dissipation

The energy dissipated by each specimen is defined as the area inside the loop of force-displacement relationship. The cumulative energy of each specimen (at 2.00% drift for comparison) are presented in Table 3. All infilled frames (specimen 2-4) dissipate more energy than that of the bare frame, which are about 1.77- 6.81 times that of specimen 1. Specimen 2 shows the highest energy dissipation which may relate roughly to the size of the infill wall. For specimen 3, frame with partial height infill wall shows the lowest energy dissipation as compared with other infilled frames. It may be corresponded with the lowest size of the infill wall and also minor damage on the infill wall. The damage of specimen 3 is concentrated on both column members above the height of the infill wall only.

3.4 **Equivalent Viscous Damping**

Equivalent viscous damping (EVD) ratio is normally used to measure energy absorption of structures [16], and this value can be evaluated from hysteretic response under fully reversed cyclic loading (see definition of Figure 5(f))). EVD ratios are depicted in Figure 5(a)-5(f), which show both EVD ratios in first and repeated cycles. A band of recommended values of the EVD ratio for linear elastic analysis with classical damping of RC structure at or just below the yield point is also overlaid for reference (7-10 % for RC structure) [17]. Additionally, the band of the drift at peak load (between the drift at maximum load for pull & push direction) of test specimens is also overlaid in the figure. This band can be defined approximately as the point just above the yield point of the system. As shown in Figure 4, just below the band of the drift at peak load, all specimens show that EVD ratio obtained somewhat agree with the recommended typical values.

3.5 Strength Degradation

Strength degradation under cyclic loading is defined as the ratio between the strength of the first cycle and that of the second cycle. As shown in Table 3, the strength degradations are about 83-97%. These results agree with that of infilled RC frames with aspect ratio 1.5 [15], which

shows the strength degradation of a mean value equal to 85 - 90 %. The strength degradations of test specimens are clearly seen after reaching the maximum load. Overall, the strength degradations of all infilled frames (specimen 2-4) are higher than that of specimen 1.

Table 3 Hysteretic characteristics of test specimens

	SP1		SP2		SP3		SP4		SP5	
	Pull	Push	Pull	Push	Pull	Push	Pull	Push	Pull	Push
$V_{max.}$ (kN)	54.35	-52.44	162.13	-170.27	72.38	-64.63	147.00	-147.38	155.22	-73.29
$D_{max.}$	3	-2.00	0.60	-0.75	1.43	-1.00	0.68	-0.36	0.45	-2.70
$V_{res.}$ (kN)	54.35	-47.54	108.36	-	35.16	-30.65	74.76	-64.47	92.65	-72.55
$D_{0.85a}$	1.25	-1.08	0.32	-0.41	0.78	-0.68	0.27	-0.27	0.32	-0.64
$D_{0.85d}$	-	-	0.98	-0.91	1.78	-1.72	1.63	-0.86	0.75	-
$K_{max.}$ (kN/m)	5944	6003	44537	35734	11066	9784	38781	34541	33834	16225
CE (kN-m)	2.92		19.88		5.15		10.91		14.28	
$V_{max} / (V_{max})_{SP1}$	1	1	2.98	3.25	1.33	1.23	2.70	2.81	2.86	1.40
$V_{res.} / (V_{res.})_{SP1}$	1	1	1.99		0.65	0.64	1.38	1.36	1.70	1.53
$\mu_{0.85}$	-	-	3.11	2.23	2.30	2.51	5.95	3.20	2.39	-
$K_{max.} / (K_{max})_{SP1}$	1	1	7.49	5.95	1.86	1.63	6.52	5.75	5.69	2.70
$CE / (CE)_{SP1}$	1		6.81		1.77		3.74		4.89	
$(V_{2nd} / V_{1st})_{ave.}$	0.96	0.95	0.89	0.87	0.91	0.91	0.86	0.88	0.90	0.94

In which V_{max} is the maximum lateral strength; $D_{max.}$ is the drift at maximum lateral strength; $V_{res.}$ is the residual lateral strength at 3.00% drift; $D_{0.85a\ /\ d.}$ is the drift on the ascending / descending envelope curve corresponding with 85% of $V_{max.}$; $K_{max.}$ is the maximum lateral stiffness; CE is the cumulative energy dissipation at 2.00% drift; $\mu_{0.85}$ is the ductility corresponding with 85% of V_{max};

$(V_{2nd} / V_{1st})_{ave.}$ is the average ratio of strength degradation.

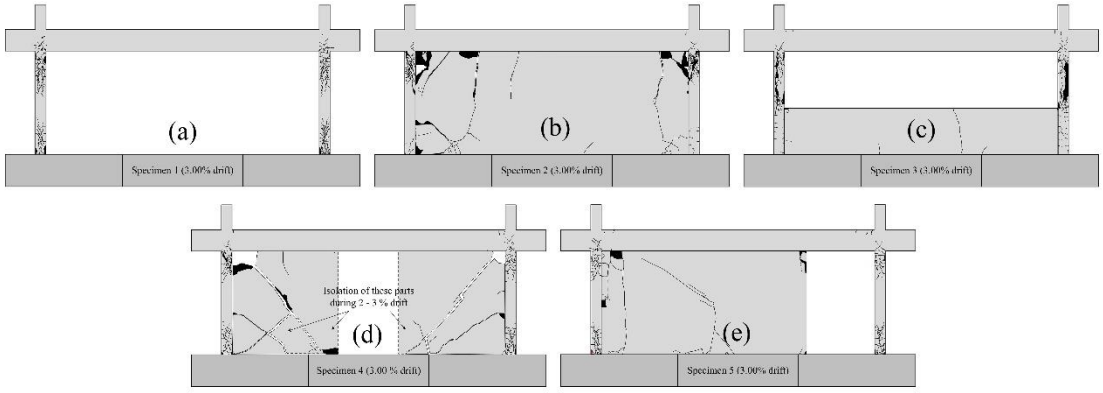

Figure 4 Crack patterns

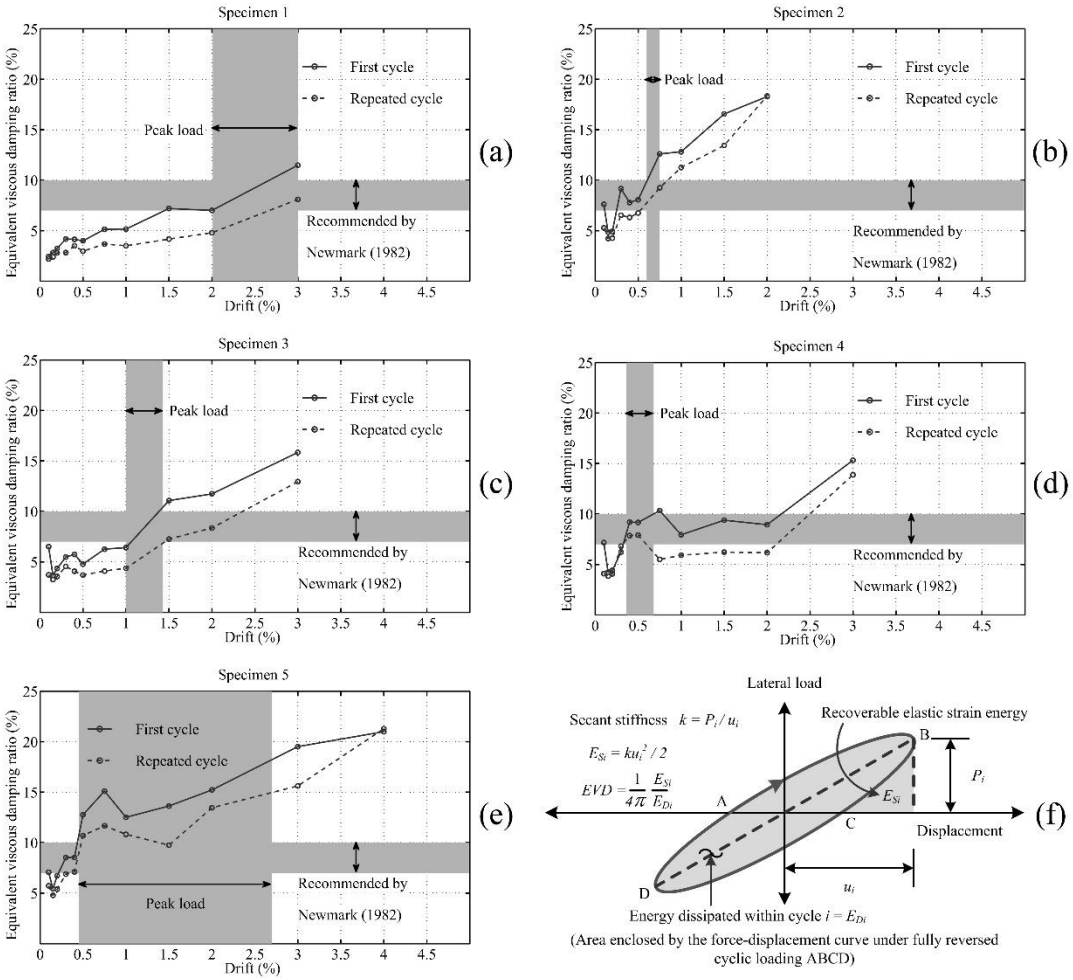

Figure 5 Equivalent viscous damping of test specimens

4 Conclusions

Results of the experimental investigation indicated that infilled walls with difference configurations significantly modify the cyclic behavior of the frame by increasing its strength (1.23-3.25 times that of bare frame), stiffness (1.63-7.49 times that of bare frame), energy dissipation (1.77-6.81 times that of bare frame), altering the force-drift relationship and ductility. However, the degree of this modification varied greatly from case to case. Furthermore, EVD ratio obtained somewhat agree with the recommended typical values for RC frames. The results strongly illustrate that infilled walls must be considered in the seismic design of new buildings and seismic evaluation of existing buildings.

As compared with infilled RC frames with low-to-moderate aspect ratio from other studies that damage on RC members is often founded on columns, beams and/or beam-column joints. While the damage on RC members of test specimens in this study is concentrated on columns only. Furthermore, it seems that drift at maximum load, ductility and strength degradation may not depend on the aspect ratio of the bounding frame. However, taking into account all the involved uncertainties, a limited number of test specimens in this study and

incomplete information of other studies, the aforementioned inspection for some parameters may be concluded roughly and mainly limited to this study.

5. References

[1] Lee HS and Woo SW. Effect of masonry infills on seismic performance of a 3-storey r/c frame with non-seismic detailing. Earthquake Engineering and Structural Dynamics. 2012; 31 : 353-378.

[2] Klingner RE and Bertero V. Earthquake resistance of infilled frames. Journal of the Structural Division. 1978; 104(ST6) : 973-989.

[3] Anil O and Altin S. An experimental study on reinforced concrete partially infilled frames. Engineering Structures. 2007; 29 : 449-460.

[4] Fardis MN, Bousias SN, Franchioni G and Panagiotakos TB. Seismic response and design of RC structures with plan-eccentric masonry infills. Earthquake Engineering and structural Dynamics. 1999; 28 : 173-191.

[5] Kaushik HB, Rai DC and Jain SK. Masonry-Infilled Reinforced Concrete Frames: A State-of-the-Art-Review. Earthquake Spectra. 2006; 22(no.4) : 961-983.

[6] Sattar S and Liel AB. Seismic performance of nonductile reinforced concrete frames with masonry infill walls-II: collapse assessment. Earthquake Spectra. 2016; 32(no.2) : 819-842.

[7] Negro P and Columbo A. Irregularities induced by nonstructural masonry panels in framed buildings. Engineering Structures. 1997; 19(7) : 576-585.

[8] Niyompanitpattana S and Warnitchai P. Effects of masonry infill walls with openings on seismic behaviour of long-span GLD RC frames. Magazine of Concrete Research. 2017; 69(21) : 1082-1102.

[9] Paulay T and Priestley MJN. Seismic design of reinforced concrete and masonry buildings. USA: John Wiley & Sons Inc; 1992.

[10] Turgay T, Durmus M, Binici B and Ozcebe G. Evaluation of the predictive models for stiffness, strength, and deformation capacity of RC frames with masonry infill walls. Journal of Structural Engineering. 2014; 140(10) DOI: 10.1061/(ASCE)ST.1943-541X.0001069.

[11] FEMA (Federal Emergency Management Agency). FEMA 461 Interim testing protocols for determining the seismic performance characteristics of structural and nonstructural components. Washington, D.C., USA. 2007.

[12] Niyompanitpattana S. Effects of Masonry Infill Walls with Different Opening Configurations on Seismic Behavior of Long-Span Gravity-Load-Designed RC Frames [Doctoral Engineering Dissertation]. Pathumthani, Asian Institute of Technology; 2017.

[13] Mehrabi AB, Shing PB, Schuller MP and Noland JL. Experimental Evaluation of Masonry-Infilled RC Frames. Journal of Structural Engineering. 1996; 122(3) : 228-237.

[14] Jin K, Choi H and Nakano Y. Experimental Study on Lateral Strength Evaluation of Unreinforced Masony-Infilled RC Frame. Earthquake Spectra. 2016; 32(3) : 1725-1547.

[15] Kakaletsis DJ and Karayannis CG. Experimental investigation of infilled reinforced concrete frames with openings. ACI Structural Journal. 2009; 106(2) : 132-141.

[16] Chopra, A.K. Dynamics of Structures: Theory and Applications to Earthquake Engineering.

Upper Saddle River, NJ: Prentice Hall; 2001.
[17] Newmark NM and Hall WJ. Earthquake spectra and design. Earthquake engineering research institute, Berkeley, California, USA; 1982.